

20 structures has been estimated as being in excess of £4 billion for the UK (Middleton 2004) and \$140
21 billion for the US (American Association of State Highway Transportation Officials 2008).
22 Deficiencies in the strength of infrastructure may be actual deficiencies arising as a result of a variety
23 of factors including: deterioration, construction defects, accidental damage, changes in understanding
24 and failure to design for future loading. Deficiencies may also be 'theoretical' deficiencies arising as a
25 result of uncertainty or the application of 'inappropriate' analytical approaches that are overly
26 conservative (Shave et al. 2007). For example, a survey of UK highway bridge infrastructure
27 (Highways Agency 2003) identified that of 272 failures by assessment of the primary structure, 73
28 were attributable to "conservative or inappropriate analysis", with a further 32 failures due to
29 "particularly conservative assumptions", sometimes as a result of incomplete design information. The
30 demolition and replacement of structures failing assessment can involve large capital expenditure;
31 environmental impacts; lengthy interruptions to service; over-burdening of nearby infrastructure; and
32 local opposition to construction works. Strengthening options may exist, however there may still be
33 considerable cost involved. If a better understanding of structural behaviour can lead to an
34 improvement in the assessment of the strength of existing structures then this is likely to be of
35 considerable economic value.

36 In reinforced concrete structures the capacity of a joint or interface to transfer shear forces may be the
37 critical consideration in assessing the capacity of the structure as a whole. Historical failures, such as
38 the failure at a half-joint or dapped-end that precipitated the 2006 collapse of the de la Concorde
39 overpass in Quebec (Gouvernement du Québec 2007), have highlighted the need for improved
40 understanding of the behaviour of critical joints subject to combinations of shear and tension. While
41 the lower bound theorem of plasticity is widely used in design of reinforced concrete, it may be
42 advantageous to use the upper bound theory for the purposes of assessment, provided suitable values
43 for the effectiveness of the concrete are included in the analysis (Ibell et al. 1997). This study provides
44 experimental verification of the upper bound theorem of plasticity for the analysis of initially
45 uncracked concrete subject to combined shear and tension. Effectiveness factors for concrete
46 indicated by the experimental results are presented.

47

RESEARCH SIGNIFICANCE

48 Considerable investigation has been undertaken into the capacity of a reinforced concrete joint or
49 interface to transfer shear load, where this load transfer is described variously as shear transfer, shear
50 friction or aggregate interlock. However, there has been very little consideration of the influence of
51 combinations of shear and tension on the reinforced concrete behaviour. This is important because in
52 many situations, such as at half-joints / dapped-ends, the shear plane will be subjected to a coexisting
53 tension, either as a matter of design or as a result of unanticipated secondary effects. This study
54 presents experimental results obtained using a 'modified' push-off testing approach to investigate
55 combinations of shear and tension. An analysis applying the plasticity theory for shear and normal
56 stresses at an interface is carried out. A number of experimental results reported in the literature are
57 also analysed. The modified push-off tests presented provide new experimental validation for the use
58 of the upper bound theory of plasticity to describe interfaces of this type, subject to combinations of
59 shear and tension. New effectiveness factors for concrete, indicated by this research, are suggested for
60 use in plastic analysis of joints.

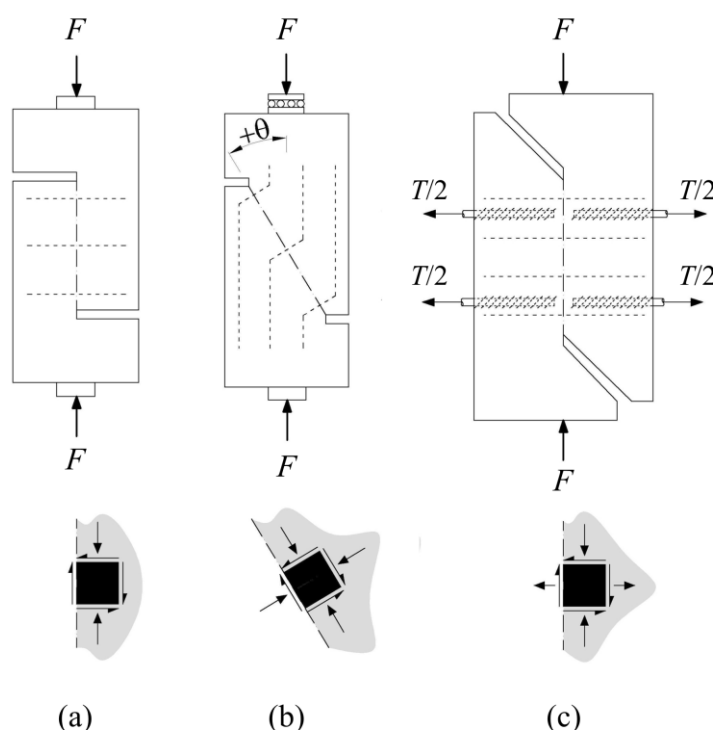
61

BASIS FOR INVESTIGATION

62 **Experimental investigations**

63 The transfer of shear across an interface has been the subject of much research. Experimental
64 investigations, notably by Hofbeck et al. (1969), Mattock & Hawkins (1972) and Walraven &
65 Reinhardt (1981), have involved the use of 'push-off' tests. Conventional push-off tests (Figure 1a)
66 are designed to elicit pure shear across an interface by forming a failure plane concentric with, and
67 parallel to, an applied load, F . Roughness of the interface due to the presence of aggregate and other
68 deviations means that, for slip of the two halves of the specimen to occur along the interface, there
69 must be sufficient crack dilation for the opposing faces either to override (Birkeland & Birkeland
70 1966), or else for the formation and rotation of diagonal 'struts' in the concrete to occur (Hofbeck et
71 al 1969). Dilation strains any reinforcement crossing the interface and commensurate restraint forces
72 are developed in turn. Such tests may involve an interface that is initially uncracked, meaning that no

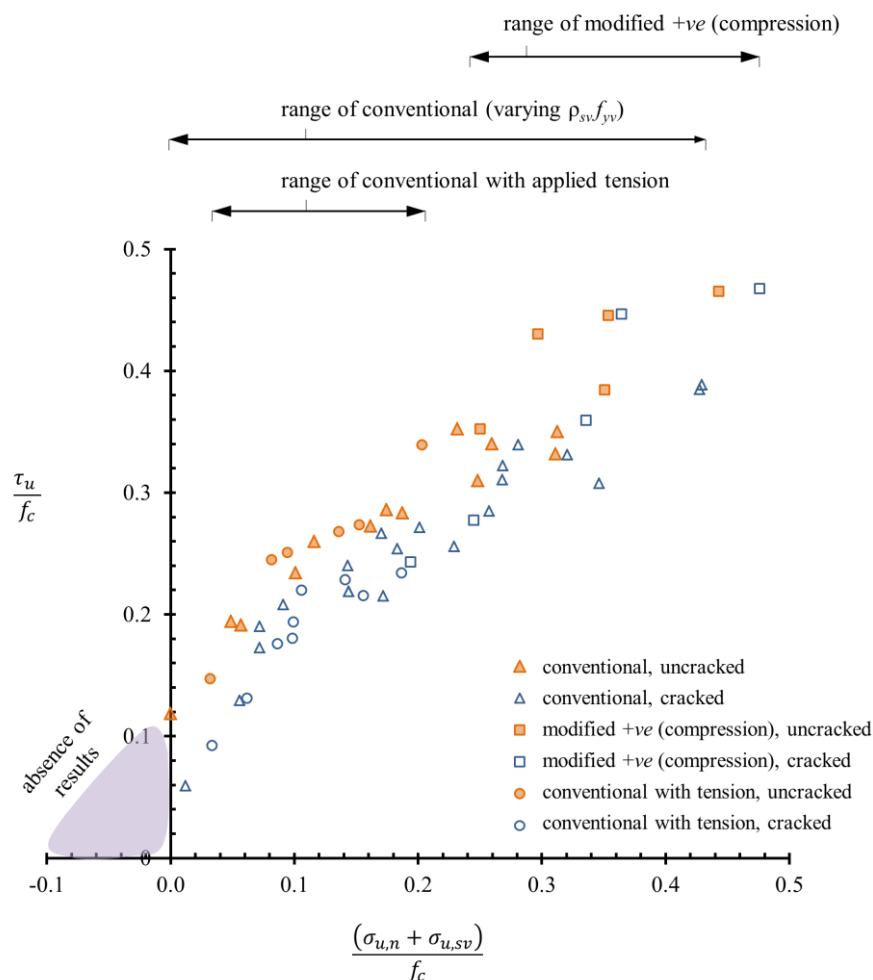
73 visible cracking of the interface is evident at the start of the test; or initially cracked, indicating that
74 visible cracking of the interface is evident. Initially cracked specimens have generally been subjected
75 to a controlled pre-cracking along the interface, usually by application of a knife edge load along the
76 edge of the intended failure plane (Hofbeck et al. 1969, Mattock & Hawkins 1972, Walraven &
77 Reinhardt 1981). It is difficult in practice to establish internal crack widths in a concrete push-off
78 specimen, meaning that the crack widths reported are typically measured externally. In the following
79 discussion of the historical results, compressive stresses normal to the interface are denoted positive in
80 accordance with the presentation of earlier investigators.



81
82 Figure 1. Push-off test arrangements and stress state at interface due to applied loads: (a) conventional; (b)
83 modified with +ve θ ; (c) conventional with tension [data from Mattock and Hawkins 1972, Mattock et al. 1975]

84 Mattock & Hawkins (1972) modified the conventional specimen geometry to produce a “modified”
85 push-off specimen (Figure 1b) that induced a diagonal failure plane (at +ve angles θ varying from 0°
86 to 75°) concentric with, but inclined to, the applied load F . This arrangement generated a failure plane
87 subject to a combination of shear, $F\cos\theta$, and a compression, $F\sin\theta$. The average compressive normal
88 stress due to the applied load ranged from 2.8 to 17 MPa for specimens noted to fail in shear (θ from

89 15° to 45°), and from 19.2 to 27.1 MPa for specimens noted to fail in compression (θ from 60° to 75°)
 90 for a range of normal strength concretes. In all cases the reinforcement was arranged perpendicular to
 91 the failure plane.



92
 93 Figure 2. Normalised push-off tests results [data from Hofbeck et al. 1969, Mattock and Hawkins 1972 and
 94 Mattock et al 1975]

95 Mattock et al. (1975) performed a series of conventional push-off tests with embedded bars
 96 perpendicular to the interface, allowing tension T to be generated across the failure plane (Figure 1c).
 97 These tests were carried out with a range of fixed tensions applied, giving an constant average tensile
 98 normal stress across the shear plane of between -0.7 and -2.8 MPa. The specimens were then
 99 subjected to increasing shear load. At peak load F_u the restraint stress provided by the reinforcement,

100 which was noted to yield, was greater than the applied tension; indicating that the net normal force on
101 the interface was compressive.

102 Figure 2 summarises normalised push-off test results carried out by Hofbeck et al. (1969), Mattock &
103 Hawkins (1972), and Mattock et al. (1975). The mean concrete compressive cylinder strength is f_c .
104 The nominal average ultimate shear stress on the shear plane of area A is τ_u where:

$$\tau_u = \frac{F_u \cos \theta}{A} \quad \text{Equation 1}$$

105 Assuming yielding of the reinforcement, the confining stress normal to the shear plane due to the
106 restraining effect of the internal steel of area A_{sv} and yield strength f_{yv} is $\sigma_{u,sv}$:

$$\sigma_{u,sv} = \frac{A_{sv} f_{yv}}{A} \quad \text{Equation 2}$$

107 The externally applied stress (compression +ve) normal to the shear plane is $\sigma_{u,n}$. For the modified
108 push-off tests:

$$\sigma_{u,n} = \frac{F_u \sin \theta}{A} \quad \text{Equation 3}$$

109 and for the conventional tests with a tensile force $-T$ applied normal to the shear plane through
110 embedded bars:

$$\sigma_{u,n} = \frac{-T}{A} \quad \text{Equation 4}$$

111 Significant overlap can be seen between the series with respect to the total restraint stress across the
112 interface presented as the sum of varying combinations of $\sigma_{u,n}$ and $\sigma_{u,sv}$. Broadly speaking, initially
113 uncracked specimens achieve higher normalised shear strengths than cracked specimens for similar
114 normalised restraint stresses. The modified specimens with +ve θ (compression) and the conventional
115 specimens with tension show relatively good agreement with the conventional results, indicating that
116 the superposition of moderate normal stresses with the passive restraint stresses due to the

117 reinforcement is not unreasonable. However, in the region in which a net tension is present across the
118 shear plane, there is an absence of experimental results. This is significant because, although the
119 contribution of concrete tensile strength is typically neglected in strength design, the pattern of results
120 indicates potential non-zero shear strength in this region for an initially uncracked interface. This
121 study therefore presents results obtained from new, modified push-off specimens with $-ve \theta$ (tension)
122 in order to provide empirical data that allows theoretical understanding to be evaluated across the full
123 range of values illustrated in Figure 2. However, it is necessary to first consider the theory.

124 **Existing models for shear transfer at an interface**

125 Models for interface shear or shear friction have been proposed by numerous investigators. A detailed
126 chronological presentation of many of these models is given by Santos & Julio (2012). Hanson (1960),
127 an early investigator, attributed the shear resistance at the contact surface of a concrete-concrete
128 interface to "adhesive bond, roughness ... and stirrups". The *fib* model code volume 1 (*fib* 2010)
129 similarly considers, "mechanical interlock and adhesion; frictional effects resulting from external
130 compression forces and/or clamping forces due to reinforcement crossing the interface; and dowel
131 action of reinforcement crossing the interface", as the three principal mechanisms influencing
132 concrete-to-concrete shear transfer behaviour. In general, existing models for shear transfer can be
133 characterised as describing some combination of these three mechanisms. Birkeland & Birkeland
134 (1966) for example proposed a friction only model with a friction angle φ , entailing a coefficient of
135 friction $\tan\varphi$:

$$\tau_u = \rho_{sv} f_{yv} \tan \varphi \quad \text{Equation 5}$$

136 while Mattock & Hawkins (1972) considered a combination of friction and an empirically determined
137 constant that accounts for any adhesive component of resistance.

$$\tau_u = 1.38 + 0.8(\sigma_{u,n} + \rho_{sv} f_{yv}) \quad \text{Equation 6}$$

138 Although a dowel contribution was recognised, it was thought to be implicitly accounted for by the
139 "fictitiously high" (Mattock & Hawkins 1972) coefficient of friction inferred from the experimental

140 results. The *fib* model code (*fib* 2010) also indicates that mechanical interlock and adhesion can be
141 expected to contribute primarily when slip displacements are very small, but that for larger slip
142 displacements these effects are likely to be substantially reduced. As a result, two governing shear
143 transfer modes are posited in the *fib* model code: rigid bond-slip behaviour associated with dominance
144 of the adhesion/interlock mechanism; and non-rigid bond-slip behaviour associated with dominance
145 of the frictional and dowel mechanisms (*fib* 2010). Thus it may be inferred that adhesion/interlock is
146 likely to be either the dominant mechanism, as in the rigid bond-slip condition, or else a rather small
147 or even negligible contributor in the non-rigid bond slip case.

148 Shear transfer models implicitly allow for permanent compressive normal stresses across an interface
149 to be superposed with the clamping force of the reinforcement, for the purposes of calculating the
150 normal force associated with the frictional component of resistance. The validity of this superposition
151 for moderate compressive stresses was shown experimentally by Mattock and Hawkins (1972).
152 However, shear friction models typically tend to zero shear strength as confining compressive stresses
153 reduce to zero, as in the friction-only model of Birkeland & Birkeland (1966) and the friction-
154 interlock-dowel model of ACI318 (ACI 2014). Alternatively, where models imply that shear strength
155 may be non-zero when normal stresses are zero, there is a cut-off specified in the case of net tension,
156 as in the models of EC2 (BSI 2004) and the *fib* model code (*fib* 2010). The modelling of actual
157 behaviour in the presence of coexisting normal tensile stresses therefore presents a challenge to these
158 models. While the assumption of zero shear strength in the presence of tension may be appropriate for
159 the purposes of interface design, shear friction models do not appear to be suitable for the
160 investigation of the actual strength of initially uncracked concrete in the presence of a net tensile
161 normal stress.

162 **Plastic analysis of shear transfer at an interface**

163 An alternative approach to the analysis of shear transfer at a cracked and uncracked concrete interface
164 is provided by the upper bound theory of plasticity. Cracked in this context is taken to mean concrete
165 having cracks visible to the naked eye, or a crack width of approximately 0.1 mm (Neville 2011).

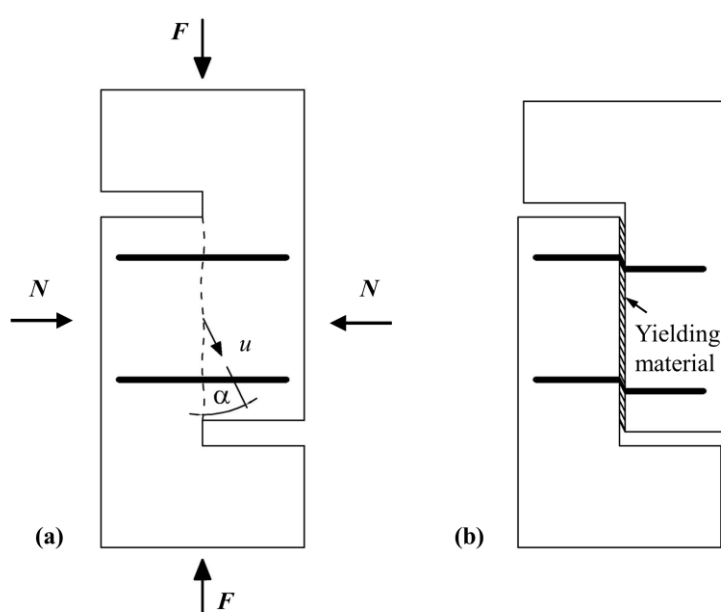
166 Where specimens are reported in the literature as being pre-cracked or visible cracking is reported
167 prior to loading, the interface is assumed to be cracked; otherwise the interface is assumed to be
168 uncracked. The theory for an uncracked interface in monolithic concrete was developed by Jensen
169 (1977). Identical solutions were obtained by Chen (1988). An upper bound analysis of a test series of
170 conventional push-off specimens with an initially uncracked interface with steel transverse
171 reinforcement was carried out by Ibell & Burgoyne (1999) assuming an S-shaped shear plane. Jensen
172 (1977) also presented a plastic analysis for a cracked interface, assuming plane strain conditions such
173 that sliding is assumed in the plane of the interface and using ad hoc effectiveness factors relating to
174 particular experimental results. The application of the theory to cracked concrete was further
175 developed by Zhang (1997) with the more general treatment of the reduced effectiveness of concrete
176 due to reduced concrete cohesion along a cracked failure plane. Comprehensive treatment of the
177 background and derivations to these approaches are provided elsewhere by Nielsen & Hoang (2011).

178 The following assumptions are made here in applying the upper bound theory of plasticity to the
179 behaviour of interfaces in reinforced concrete:

- 180 1. Perfectly plastic material behaviour is assumed such that strains prior to yielding of the
181 material are negligible, and strains thereafter may be arbitrarily large.
- 182 2. An effectiveness factor v for concrete in compression is applied such that the effective
183 concrete strength in compression is vf_c , where f_c is the uniaxial concrete compressive cylinder
184 strength. This is intended to account for a number of effects including softening, micro-
185 cracking and local stress concentrations (Nielsen & Hoang 2011).
- 186 3. A further effectiveness factor v_s is applied to the strength of cracked concrete such that the
187 effective strength of cracked concrete against 'sliding' is v_svf_c . This accounts for the reduced
188 yield strength of concrete along a cracked plane. A value of 0.5 is adopted for v_s , following
189 Zhang (1997).
- 190 4. A Modified-Coulomb failure criterion for concrete is adopted. The concrete is treated as a
191 granular material with a friction angle ϕ of 37° under all combinations of stress (Nielsen &

192 Hoang 2011). The value of ϕ is assumed to be the same for both uncracked and cracked
193 concrete (Zhang 1997). A limiting concrete tensile strength f_t is assumed to account for the
194 possibility of separation failure. The value of f_t is taken as $v_t v_f c$, where v_t is a further
195 effectiveness factor for concrete in tension.

196 5. Steel reinforcing bars are assumed to carry only axial forces and yield at stress f_{yv} . Dowel
197 action of reinforcement is not explicitly considered, although its influence will be to some
198 extent implicit in any values of effectiveness factors inferred from experimental results.



199
200 Figure 3. Conventional push-off test as an example of an interface subject to shear: (a) with displacement vector
201 u at angle α to the applied load; (b) highlighting the deformation due to yielding of material at the interface

202 Two cases are thus considered in the following analyses in relation to the transfer of shear across an
203 interface in reinforced concrete:

- 204 1. An initially uncracked interface in which the effective yield strength of the concrete material
205 is the same in all directions;
- 206 2. An initially cracked interface in which the effective yield strength of the concrete is reduced
207 in the plane of the cracked interface.

208 The formulation used for the plastic analysis is presented with respect to a conventional push-off test
209 with reinforcement perpendicular to the interface as shown in Figure 3. The interface has an area A . A
210 force F is applied parallel to the interface generating shear stresses $\tau = F/A$ parallel to the interface
211 and a force N is applied perpendicular to the interface generating normal stresses $\sigma_n = N/A$. Note that
212 N is denoted positive for compression. Relative movement of the two halves of the push-off test is a
213 displacement vector u at an angle α to the interface and the applied load. The reinforcement ratio ρ_{sv} is
214 the area of transverse steel A_{sv} divided by the area of the interface. The transverse reinforcement is
215 thus considered as smeared across the failure plane.

216 **Uncracked monolithic concrete interface**

217 Following an upper bound approach, the work done by the displacement of the external loads W_E is
218 equated to the energy dissipated internally W_I by yielding mechanisms. Energy dissipation in the
219 push-off test arrangement is thus the sum of the energy dissipated by yielding of the concrete along
220 the interface and the energy dissipated by yielding of the transverse reinforcement in the axial
221 direction by displacement $u \sin \alpha$. Defining:

$$\psi = \frac{\rho_{sv} f_{yv}}{v f_c} \quad \text{Equation 7}$$

$$\psi^* = \psi + \frac{N}{A v f_c} \quad \text{Equation 8}$$

222 The external work W_E done by the applied loads is the sum of the work done by the applied load F in
223 the vertical direction and the work done against the restraint force N normal to the interface;

$$W_E = F u \cos \alpha - N u \sin \alpha \quad \text{Equation 9}$$

224 The energy dissipated by the yielding reinforcement $W_{I,r}$, assumed to be axial and neglecting dowel
225 action is;

$$W_{I,r} = A_{sv} f_{yv} u \sin \alpha \quad \text{Equation 10}$$

226 The energies dissipated by the yielding concrete $W_{I,c}$ for displacements at angles α relative to the
 227 interface of less than, equal to, or greater than, the friction angle φ are;

$$W_{I,c} = \frac{1}{2} v f_c u (1 - \sin \alpha) A \quad \text{for } 0 < \alpha \leq \varphi \quad \text{Equation 11}$$

$$W_{I,c} = \frac{1}{2} v f_c u (1 - \sin \varphi) A \quad \text{for } \alpha = \varphi \quad \text{Equation 12}$$

$$W_{I,c} = \left(\frac{1}{2} v f_c (1 - \sin \alpha) + \left(\frac{\sin \alpha - \sin \varphi}{1 - \sin \varphi} v_t v f_c \right) \right) u A \quad \text{for } \alpha > \varphi \quad \text{Equation 13}$$

228 for an arrangement analogous to that shown in Figure 3. Note that for $\alpha >$ the friction angle φ , there is
 229 a component of dissipation due to separation of the concrete, governed by the effective concrete
 230 strength in tension $v_t v f_c$. If the effective concrete tensile strength is assumed to be negligible, i.e. $v_t =$
 231 0, then no energy is dissipated by the concrete in tension and Equation 13 reduces to Equation 11.

232 Thus minimising for τ/f_c , for an uncracked interface in monolithic concrete, Nielsen and Hoang (2011)
 233 show that:

$$\frac{\tau}{f_c} = \sqrt{(\psi^* + v_t) \left[v - 2v_t \frac{\sin \varphi}{1 - \sin \varphi} \right] - (\psi^* + v_t)} \quad \text{Equation 14}$$

234 for,

$$\psi^* \leq v \frac{1 - \sin \varphi}{2} - v_t (1 + \sin \varphi) \quad \text{Equation 15}$$

235 and,

$$\frac{\tau}{f_c} = v \frac{1 - \sin \varphi}{2 \cos \varphi} + \psi^* \tan \varphi \quad \text{Equation 16}$$

236 for,

$$v \frac{1 - \sin \varphi}{2} - v_t(1 + \sin \varphi) \leq \psi^* \leq v \frac{1 - \sin \varphi}{2} \quad \text{Equation 17}$$

237 and,

$$\frac{\tau}{f_c} = \sqrt{\psi^*(v - \psi^*)} \quad \text{Equation 18}$$

238 for,

$$v \frac{1 - \sin \varphi}{2} \leq \psi^* \leq \frac{v}{2} \quad \text{Equation 19}$$

239 and,

$$\frac{\tau}{f_c} = \frac{v}{2} \quad \text{Equation 20}$$

240 for,

$$\psi^* \geq \frac{v}{2} \quad \text{Equation 21}$$

241 Equation 20 provides a limiting shear strength occurring when $\alpha = 0$. In this case the displacement
242 vector u is parallel to the interface with no component of displacement in the axial direction of the
243 transverse reinforcement, meaning that all energy dissipation is by yielding of the concrete. Such an
244 interface can thus be thought of as locked-up or over-reinforced, as observed experimentally by
245 Mattock & Hawkins (1972).

246 **Cracked concrete interface**

247 In a similar manner, the work done and energy dissipated can be equated for an arrangement
248 analogous to that shown in Figure 3 for a cracked interface. This condition may occur at a joint or at a
249 pre-existing macro-crack in the web of a concrete beam. For a cracked interface, conditions of plane
250 strain are assumed such that the angle α of the displacement vector u is not less than the friction angle

251 φ . Nielsen and Hoang (2011) show that minimising for τ/f_c and incorporating the effectiveness factor
 252 v_s for the reduced strength of cracked concrete gives:

$$\frac{\tau}{f_c} = \sqrt{(\Psi^* + v_s v_t) \left[v_s v - 2v_s v_t \frac{\sin \varphi}{1 - \sin \varphi} \right] - (\Psi^* + v_s v_t)} \quad \text{Equation 22}$$

253 for,

$$\Psi^* \leq v_s v \frac{1 - \sin \varphi}{2} - v_s v_t (1 + \sin \varphi) \quad \text{Equation 23}$$

254 and,

$$\frac{\tau}{f_c} = v_s v \frac{1 - \sin \varphi}{2 \cos \varphi} + \Psi^* \tan \varphi \quad \text{Equation 24}$$

255 for,

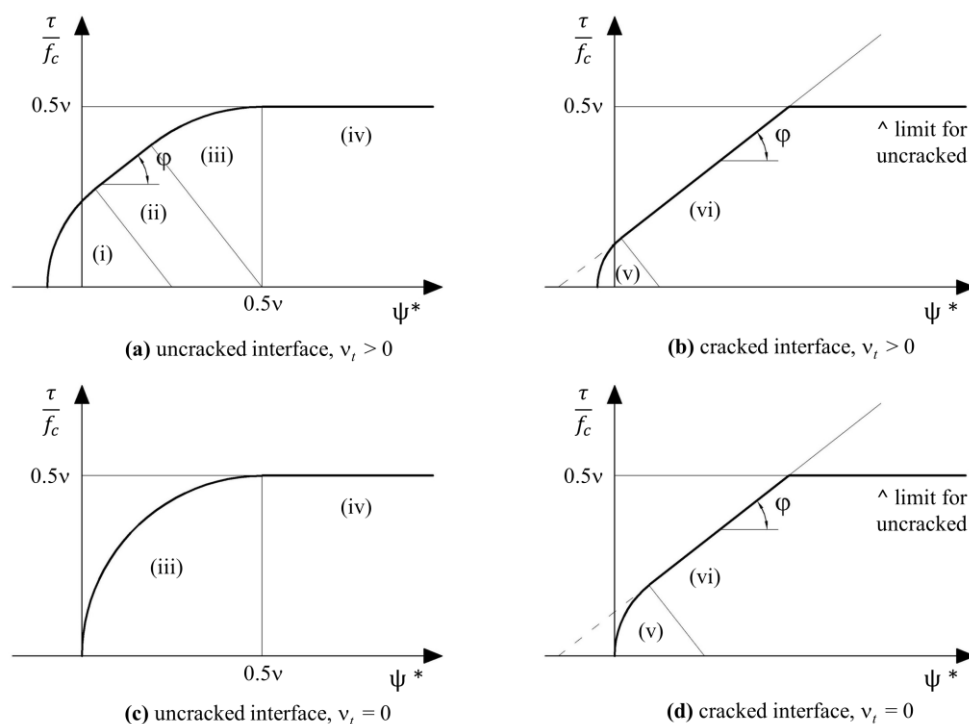
$$\Psi^* \geq v_s v \frac{1 - \sin \varphi}{2} - v_s v_t (1 + \sin \varphi) \quad \text{Equation 25}$$

256 The capacity of the cracked interface is subject to the further limiting condition that it cannot exceed
 257 the capacity of an uncracked interface. This condition is logical since there is no reason why a cracked
 258 plane should be stronger than uncracked material and, in any such case, failure would simply be
 259 expected to occur through the uncracked material immediately adjacent to the cracked plane. This
 260 condition is also in accordance with the observations of Mattock & Hawkins (1972) that there was no
 261 difference in the shear capacity of initially cracked and initially uncracked specimens with high levels
 262 of transverse reinforcement or subject to large compressive normal stresses.

263 The equations of the plastic analysis lead to the non-dimensional shear capacity envelopes drawn in
 264 Figure 4. The envelopes for cracked and uncracked interfaces are shown for $v_t = 0$, assuming that the
 265 effective strength of concrete in tension is negligible; and for $v_t > 0$, assuming that the effective
 266 concrete strength in tension is non-zero but small compared to the effective concrete strength in

267 compression. Parts i, ii, iii, iv, v and vi of the envelopes shown in Figure 4 are governed by Equations
 268 14, 16, 18, 20, 22 and 24 respectively.

269 Figure 4 highlights the influence of the effective concrete tensile strength for small values of net
 270 normal stress across the interface ψ^* . Although the equations of the cracked plastic analysis are valid
 271 for $v_t > 0$, it would be unusual to consider a non-zero concrete tensile strength at a cracked interface,
 272 as a crack width greater than approximately 0.1 mm is typically associated with a complete loss of
 273 concrete tensile strength (Nielsen & Hoang 2011). The following analysis thus adopts the envelopes
 274 shown in Figure 4 for uncracked interfaces assuming $v_t > 0$ (Figure 4a); and for cracked interfaces
 275 assuming $v_t = 0$ (Figure 4d).

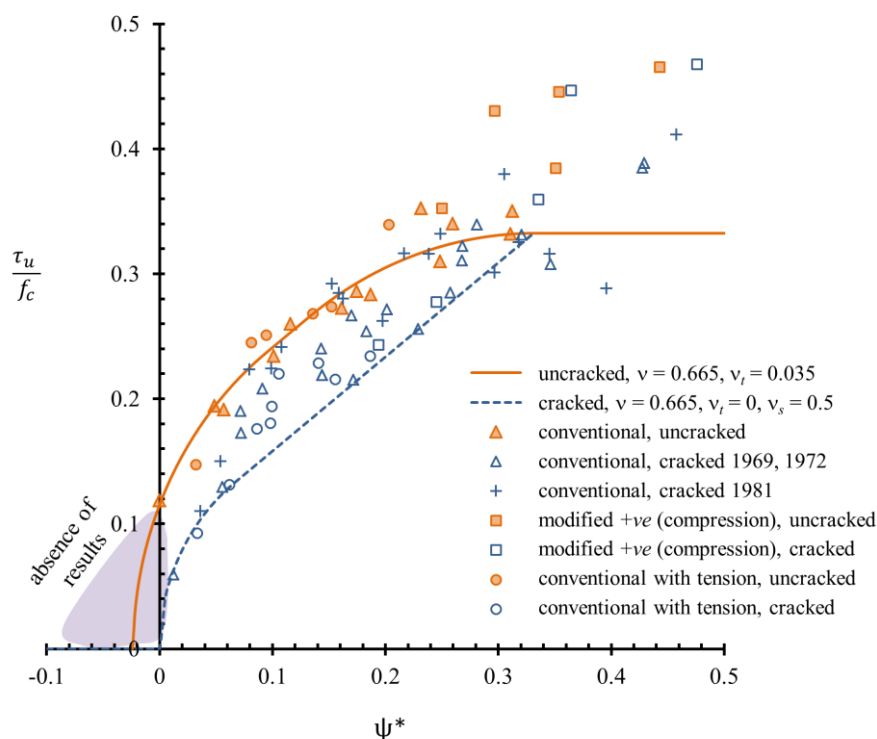


276
 277 Figure 4. Non-dimensional shear capacity envelopes for uncracked and cracked interfaces for $v_t > 0$ and $v_t = 0$

278 Comparison with results from the literature

279 Chen (1988) proposed effectiveness factors for concrete of $v = 0.665$ and $v_t = 0.035$ for the upper
 280 bound plastic analysis of an uncracked interface based on comparison with the conventional push-off
 281 testing results of Hofbeck et al. (1969). Chen did not carry out a commensurate analysis for a cracked

282 interface. An analysis for an uncracked interface using Chen's (1988) proposed effectiveness factors v
 283 $= 0.665$ and $v_t = 0.035$; and for a cracked interface using Chen's (1988) value of $v = 0.665$, $v_t = 0$, and
 284 Zhang's (1997) value of $v_s = 0.5$, is shown in Figure 5.



285

286 Figure 5. Uncracked analysis following the proposed v and v_t values of Chen (1988) and the commensurate
 287 cracked analysis, compared with a range of push-off test results in the literature

288 Also shown in Figure 5 is an expanded data set of initially uncracked and initially cracked:
 289 conventional push-off test results from Hofbeck et al (1969) and Walraven & Reinhardt (1981);
 290 modified push-off tests with compression by Mattock and Hawkins (1972); and conventional push-off
 291 tests with tension from Mattock et al. (1975). Relatively good agreement is seen for the uncracked
 292 analysis for the range of applied compressive and tensile normal stresses used in these tests, although
 293 the concrete effectiveness is underestimated at higher levels of compression. This underestimation is
 294 most likely a result of increased confinement due to the strong compression field. There is a notable
 295 absence of experimental results provided in the literature for the region $\psi^* < 0$, indicating an absence
 296 of verification of the plastic theory in this region. Although there is considerable scatter, the cracked
 297 analysis generally provides a good lower bound on values until a ψ^* of approximately 0.3 is reached.

298 Many of Walraven and Reinhardt's 1981 initially cracked test results follow the uncracked curve
299 more closely than the cracked curve, particularly in the range $0.1 < \psi^* < 0.3$. This may indicate that
300 the pre-cracking procedure in this case led to internal crack widths smaller than those measured at the
301 concrete surface.

302 It would appear that there is an absence of experimental results for push-off specimens with a shear
303 plane subjected to a coexisting net tension. However, the upper bound plastic analysis (Figure 5)
304 indicates that, for an interface that is not initially cracked and having transverse reinforcement normal
305 to the failure plane, there is potentially non-zero shear strength in the region of net tension. An
306 experimental programme was carried out as part of this study in order to investigate actual behaviour
307 in this region.

308 **EXPERIMENTAL INVESTIGATION**

309 **Specimen design**

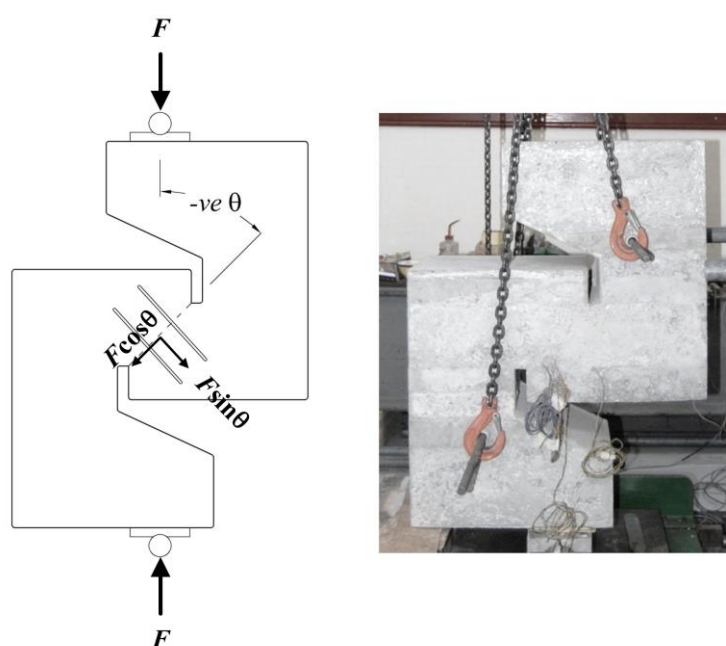
310 In order to investigate the case of a net tension across the shear plane comparable to the modified
311 push off testing approach of Mattock & Hawkins (1972), a failure plane at a $-ve$ angle θ is required. A
312 modification to the geometry of the push-off specimen (Figure 6) was thus developed previously by
313 the authors (Foster et al. 2016) in order to generate an interface subject to a combination of shear,
314 $F\cos\theta$, and tensile normal force, $F\sin\theta$ and a number of specimens with $\theta = -45^\circ$ were tested.

315 The experimental programme described below extends this approach to specimens with a range of
316 values of $-ve$ values of θ in order to provide experimental evidence of the effect of varying
317 combinations of shear and tension on the interface.

318 **Test programme**

319 Seven reinforced concrete modified push-off specimens with a range of $-ve$ values of θ were used in
320 this study (Figure 7). The breadth (being the dimension into the page for Figure 7) of all specimens
321 was 250 mm. The geometry of the specimen was varied to obtain the desired failure plane inclination.

322 The applied load in all cases was aligned concentric with the shear plane, which had length 200 mm
323 and breadth 250 mm for all specimens. For the end blocks, substantial deformed high yield internal
324 reinforcement was provided to carry forces through the two halves of the specimen and to ensure
325 failure through the plane under investigation. This reinforcement did not cross the shear plane. The
326 full end block details for specimens with $\theta = -45^\circ$ are reported by Foster et al. (2016). The end block
327 details for the specimens with $\theta = -37.5^\circ, -30^\circ, -22.5^\circ$ and -15° used in this study were detailed in a
328 similar manner.

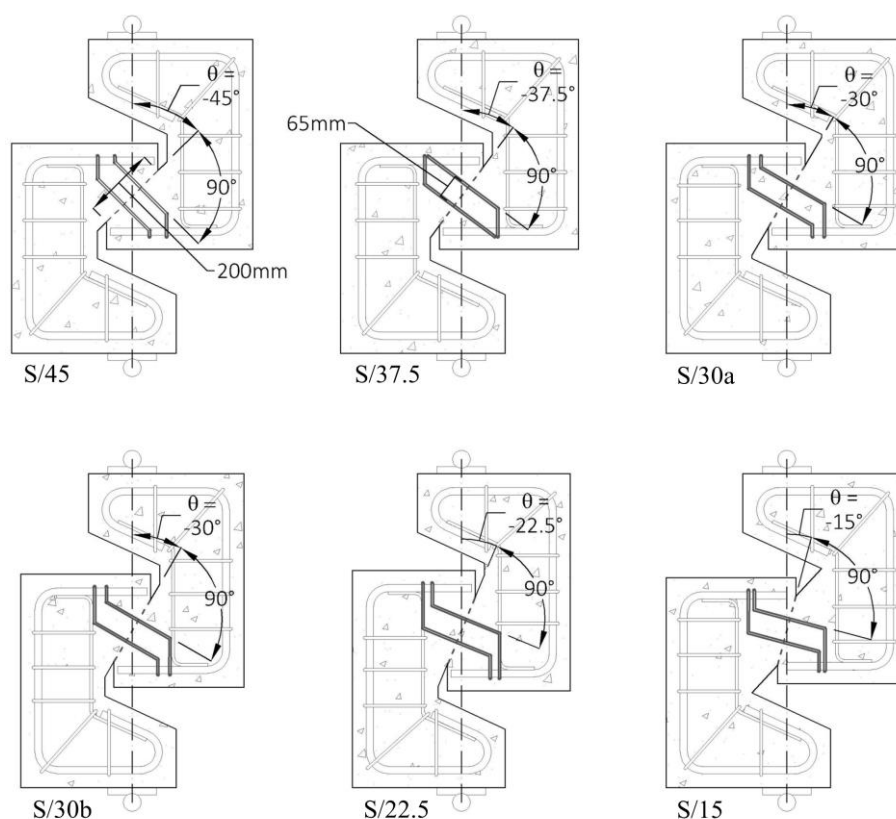


329

330 Figure 6. Modified push-off test with -ve angle θ of the type used for this investigation

331 The internal steel test reinforcement crossing the shear plane was 6 mm diameter deformed high yield
332 bar, in the form of full stirrups oriented perpendicular to the shear plane. The transverse reinforcement
333 area and spacing of 65 mm (Figure 7) was the same for all specimens, giving a $\rho_{sv} = 0.23\%$. The
334 material properties for the stirrup steel obtained by direct tensile testing were: a Young's modulus of
335 203 GPa, a 0.1% offset yield strength f_{yv} of 600 MPa and an ultimate tensile strength of 648 MPa.
336 Strain gauges were affixed to each leg of the steel test reinforcement approximately at the position of
337 the anticipated failure plane. Strain gauging of reinforcement local to the failure plane can affect the
338 local bond of the reinforcement and may therefore influence secondary transfer mechanisms, such as

339 those posited by Walraven and Reinhardt (1981), that might result from crack bridging. However, for
340 the purposes of the present study it was preferable to measure strains as close to the failure plane as
341 possible in order to obtain accurate restraint forces across the interface.



342

343 Figure 7. Modified push-off test arrangements; specimen geometry varies to obtain the intended failure plane
344 inclination; in all cases the shear plane is 200 x 250 mm; transverse reinforcement crosses the shear plane at 90°
345 and the reinforcement area and spacing are the same in each specimen

346 The concrete mix consisted of local coarse aggregate (12 mm maximum size), fine aggregate and
347 ordinary Portland cement (CEM II 32.5). Concrete 100 mm cube compressive strengths at testing are
348 shown in Table 1. The specimens were cast on their sides in timber formwork which was removed
349 approximately 24 hours after casting. Specimens were then cured in air alongside their respective test
350 cubes at ambient laboratory temperature.

351 Specimens were loaded concentrically through pinned supports in a 5000 kN Amsler column testing
352 rig. Tests were operated under displacement control. Each test began with specimens initially
353 uncracked and loaded until peak load associated with cracking of the shear plane was reached and a

354 drop in load was observed. This load is considered to be the capacity of the 'uncracked' specimen and
355 is denoted F_u . The specimen would then be substantially unloaded before being reloaded in order to
356 observe the behaviour of the cracked shear plane. The peak load obtained during reloading is
357 considered to be the capacity of the 'cracked' specimen and is denoted $F_{u,cr}$. This methodology differs
358 somewhat from the knife-edged pre-cracking methodologies reported in the literature and has two
359 distinct advantages: the first being the improved economy of testing due to the ability to obtain an
360 uncracked and a cracked capacity from a single specimen; the second being that the 'pre-cracking' is
361 applied in the same manner as the actual anticipated loading rather than by a separate and somewhat
362 unrealistic transverse loading case. A disadvantage of approach adopted here is that the width of the
363 initial crack is not controlled.

364 Table 1: Test specimens

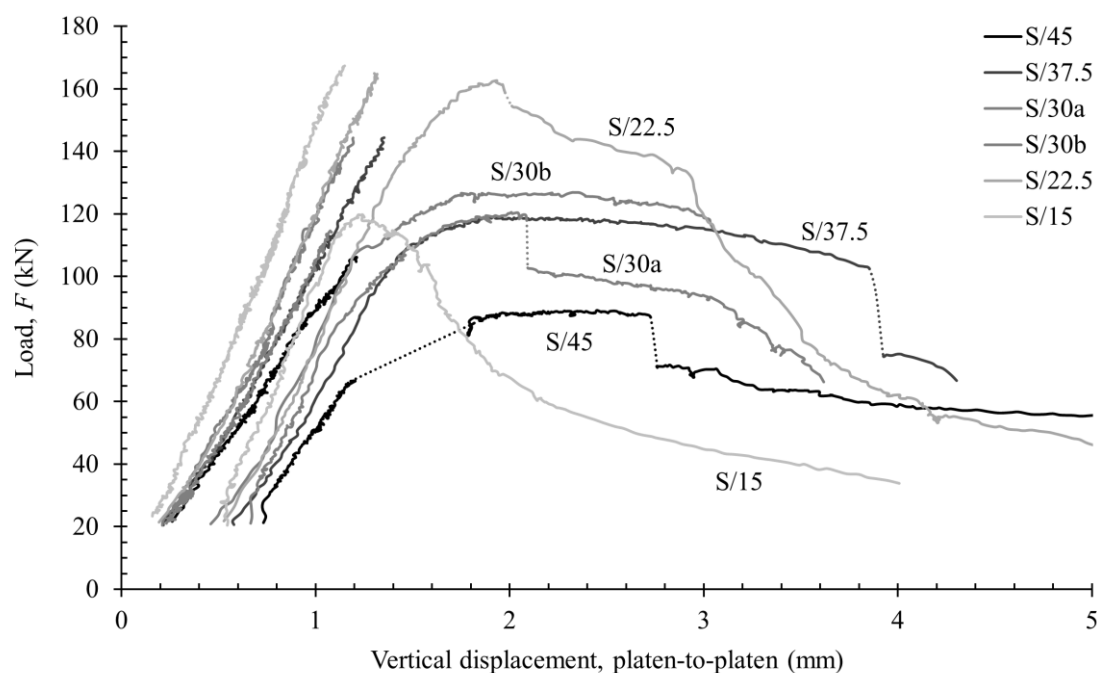
| Specimen | f_{cu} [MPa] | θ | ρ_{sv} % |
|----------|-------------------|----------|------------------|
| S/45 | 50.9 | -45.0° | 0.23 |
| S/37.5 | 64.5 | -37.5° | 0.23 |
| S/30a | 58.2 | -30.0° | 0.23 |
| S/30b | 66.4 | -30.0° | 0.23 |
| S/22.5 | 62.4 | -22.5° | 0.23 |
| S/15 | 57.1 | -15.0° | 0.23 |

365

366 EXPERIMENTAL RESULTS AND DISCUSSION

367 Figure 8 shows the load F plotted against the vertical displacement of the whole specimen measured
368 platen-to-platen. The unloading phase is omitted for here for clarity. The full load-displacement curve
369 is included in the test data associated with this paper. Initial loading of the uncracked specimen
370 elicited approximately linear elastic behaviour in the specimen prior to peak uncracked load F_u
371 followed by initial cracking of the shear plane and an abrupt drop in load. Specimens were then
372 unloaded to below approximately 20 kN (not shown) before reloading. Upon reloading the cracked
373 shear plane displayed linear behaviour until a displacement approximately equal to that previously

374 reached at cracking, but at a reduced load. Progressive reduction in stiffness was then observed with
375 increasing load until the peak load sustained by the cracked specimen $F_{u,cr}$ was reached. More ductile
376 behaviour was seen after cracking for the specimens with a less vertical crack inclination. The
377 behaviour of S/15 after cracking did not appear to correspond with the trend of increasing post-
378 cracked strength with more vertical crack inclination observed in the other tests. The shear plane
379 formed in this specimen deviated from the intended position quite considerably, indicating that the
380 non-test portion of the specimen design was not entirely suitable for this inclination. However, given
381 that by definition the intended failure plane cannot have been less strong than the deviated plane taken,
382 the stress state at the intended failure plane thus remains useful data for evaluating the upper bound
383 plastic analysis.



384

385 Figure 8. Load F plotted against vertical displacement of the whole specimen measured platen-to-platen
386 (unloading phase omitted for clarity)

387 The experimental results are summarised in Table 2. Stresses τ_u and σ_u are the nominal shear and
388 normal stresses on the interface at F_u . The stress $\sigma_{u,sv}$ is the restraining stress on the interface provided
389 by the steel reinforcement, calculated from the strains measured by the strain gauges on the steel

390 reinforcement at F_u . The stresses $\tau_{u,cr}$, $\sigma_{u,cr}$ and $\sigma_{u,cr,sv}$ are the corresponding stresses at $F_{u,cr}$. Note that
 391 tension is denoted $-ve$. The concrete compressive cylinder strength f_c is determined as:

$$f_c = 0.8f_{cu} \quad \text{Equation 26}$$

392 The strain gauge readings at peak load for F_u indicated that strains in the steel were relatively small,
 393 meaning that the force in the steel was also relatively small. The measurement of small strains in the
 394 steel is compatible with the observation that the concrete was uncracked at F_u . In all cases the
 395 interface was subject to a net normal tension at F_u . At the peak load for the cracked interface $F_{u,cr}$, the
 396 strain gauge results indicate that the steel reinforcement had in almost all cases fully yielded. In most
 397 cases the interface was subject to a net normal compression at $F_{u,cr}$. In all cases the net normal stress
 398 was near zero, indicating that in the cracked condition the applied load was approximately equal to the
 399 force in the reinforcement.

400 Table 2: Test results, note that tension is denoted $-ve$

| Specimen | F_u [kN] | τ_u / f_c | $(\sigma_u + \sigma_{u,sv}) / f_c$ | $F_{u,cr}$ [kN] | $\tau_{u,cr} / f_c$ | $(\sigma_{u,cr} + \sigma_{u,cr,sv}) / f_c$ |
|----------|---------------|----------------|------------------------------------|--------------------|---------------------|--------------------------------------------|
| S/45 | 106.2 | 0.037 | -0.034 | 75.0 | 0.031 | 0.002 |
| S/37.5 | 144.4 | 0.044 | -0.031 | 119.0 | 0.037 | -0.002 |
| S/30a | 114.6 | 0.043 | -0.023 | 120.5 | 0.045 | 0.003 |
| S/30b | 144.3 | 0.047 | -0.026 | 126.9 | 0.041 | 0.002 |
| S/22.5 | 164.9 | 0.061 | -0.024 | 162.6 | 0.060 | 0.002 |
| S/15 | 167.3 | 0.071 | -0.019 | 119.8 | 0.051 | 0.004 |

401
 402 Since the steel in these tests is observed not to yield prior to F_u , it would be inappropriate to assume a
 403 restraint stress due to the reinforcement of $\rho_{sv}f_{yv}$ for the uncracked condition. The reinforcement
 404 parameter ψ is thus replaced with a ψ' leading to a revised restraint stress parameter ψ'^* based on the
 405 actual reinforcement stress σ_{sv} in cases where reinforcement has not yielded at peak load and noting
 406 that for this arrangement the force N normal to the interface due to the specimen geometry is $F\sin\theta$:

$$\psi' = \frac{\rho_{sv}\sigma_{u,sv}}{f_c} \quad \text{Equation 27}$$

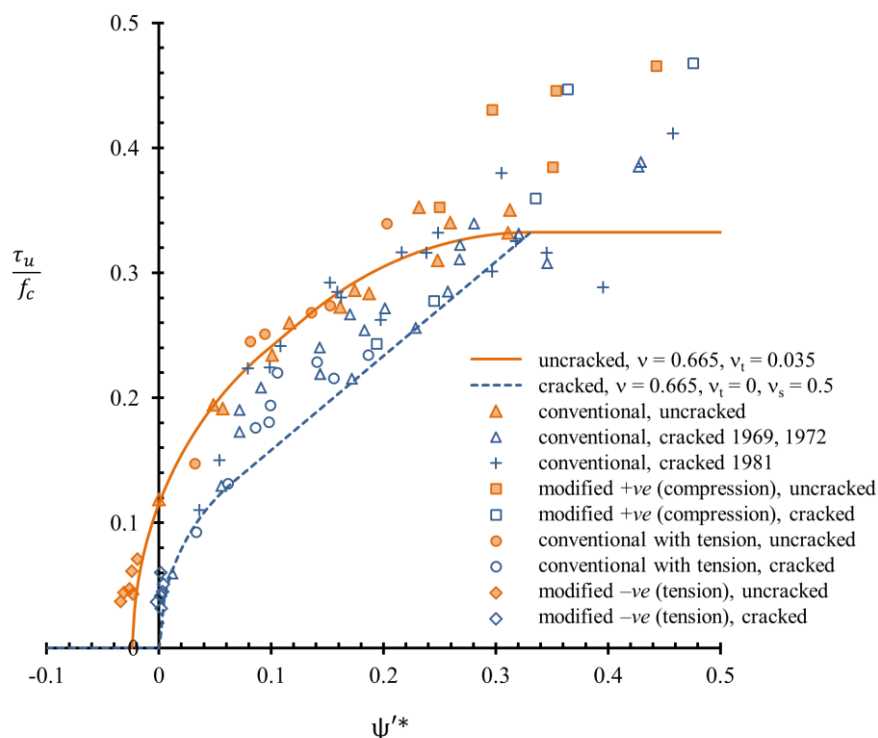
$$\psi'^* = \psi' + \frac{N}{Af_c} \quad \text{Equation 28}$$

407 While the introduction of $\sigma_{sv} < f_{yv}$ may appear incongruous with respect to a plastic analysis, it must
408 be recognised that the upper bound theorem of plasticity is used here to evaluate the stress state
409 causing failure at the concrete interface. The push-off test results are used to obtain measured
410 combinations of shear and normal stresses at the interface at failure for the purposes of verification of
411 the plastic analysis. Knowledge of σ_{sv} , inferred from the strain gauge readings provides the magnitude
412 of the restraint stress normal to the interface at failure. In fact, the small strains measured in the
413 reinforcement at F_{us} , i.e. prior to cracking, mean that the use of σ_{sv} has little effect on the analysis in
414 the cases considered here. More generally, whether it is reasonable *in design* to assume yielding of the
415 reinforcement for a given combination of applied normal and shear stresses prior to failure such that
416 f_{yv} may be used for the purposes of calculating the restraint stress component is an important question
417 and may depend on the particular case considered. However, the absence of yielding prior to peak
418 uncracked load in many of the specimens tested as part of this study indicates that this assumption
419 would not be reasonable where an interface is considered as uncracked in the presence of tension.
420 This indicates that in the presence of net normal tension, the uncracked capacity of a concrete should
421 not be superposed with a steel reinforcement contribution that assumes yielding of the reinforcement.

422 Figure 9 shows the existing range of push-off test results, with the addition of the uncracked modified
423 push-off tests with tension as a result of *-ve* angles of θ . A relatively good agreement is seen between
424 the push-off test results for shear and coexisting net tension, with the predictions of the plastic
425 analysis adopting the effectiveness factors proposed by Chen (1988).

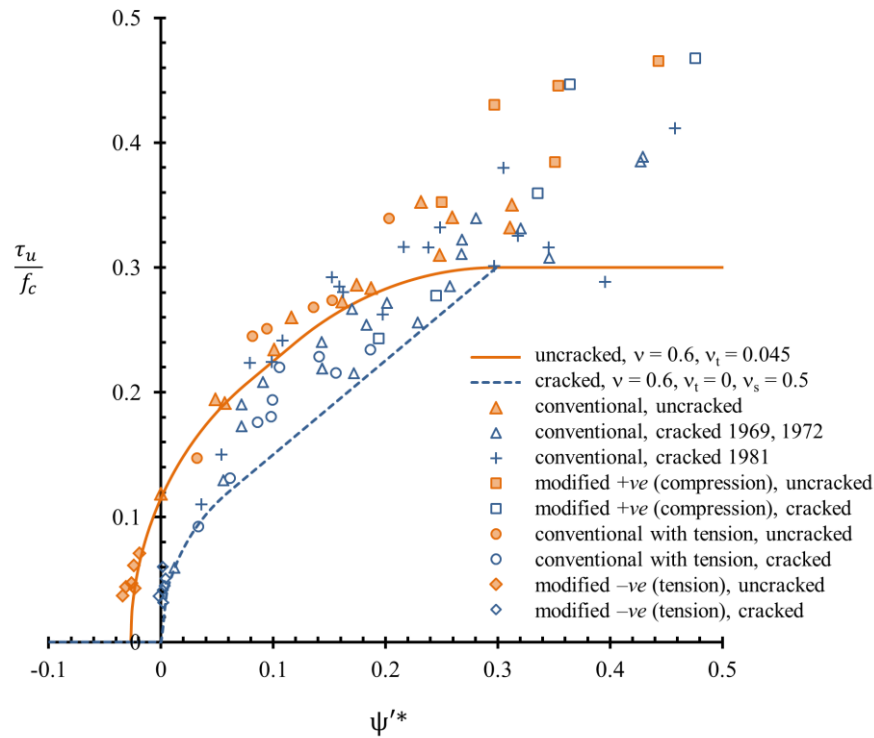
426 Although the effectiveness factors proposed by Chen (1988) have been shown to provide relatively
427 good agreement, the comparison with an expanded set of push-off tests reported subsequently in the
428 literature, and the new modified push-off test results, indicate that new effectiveness factors may be
429 appropriate. For a concrete effectiveness factor in compression of $v = 0.6$; and concrete effectiveness

430 factors in tension of $v_t = 0.045$ for uncracked concrete, and $v_t = 0$ and $v_s = 0.5$ for cracked concrete,
 431 the plastic predictions are shown in Figure 10. These values eliminate almost all of the unconservative
 432 predictions while closely following the pattern of results. For heavily reinforced specimens or those
 433 with high applied normal stresses, i.e., ψ'^* greater than approximately 0.2, the results are consistently
 434 under predicted.



435
 436 Figure 9. Uncracked analysis following the proposed v and v_t values of Chen (1988), and the commensurate
 437 cracked analysis, compared with a range of push-off test results in the literature and the new modified –ve
 438 results obtained in this study

439 It should be noted that the push-off tests reported in the literature and in this investigation cover only
 440 a limited range of sizes of shear plane. Since the plastic analysis presented does not explicitly consider
 441 the effect of shear plane size, further experimental work is required in order to determine whether the
 442 effectiveness factors indicated by the test results considered here are applicable to larger concrete
 443 interfaces of a similar type.



444

445 Figure 10. Uncracked and cracked analysis considering the proposed v and v_t values compared with a range of
 446 push-off test results in the literature and the new modified with tension results obtained in this study

447

SUMMARY AND CONCLUSIONS

448 A series of modified push-off tests with a range of $-ve$ angles θ were carried out in order to
 449 investigate the effect of varying combinations of shear and normal tension across a joint or interface
 450 in reinforced concrete. These tests, in conjunction with a number of tests reported in the literature
 451 were compared with the results of an analysis based upon the upper bound theorem of plasticity for
 452 interfaces in reinforced concrete. The following conclusions are indicated by the results of this study:

- 453 1. Modified push-off testing with varying $-ve$ angles θ provides an effective method for
 454 investigating the effect of combined shear and tension stresses on the capacity of a joint or
 455 interface in reinforced concrete.
- 456 2. A plastic analysis based upon the upper bound theorem of plasticity provides a promising
 457 method for evaluation of the strength of both cracked and uncracked interfaces in reinforced
 458 concrete subject to combined shear and normal stresses. The modified push-off test results

459 presented here provide an empirical verification of the application of the theory to interfaces
460 subject to combined shear and tension.

461 3. The push-off test results indicate that a concrete effectiveness factor in compression of $v =$
462 0.6; and concrete effectiveness factors in tension of $v_t = 0.045$ for uncracked concrete and $v_t =$
463 0 for cracked concrete may be appropriate for plastic analysis.

464 4. For interfaces subject to quite high levels of restraint, i.e. approximately $\psi'^* > 0.3$, capacity is
465 often considerably under predicted by the plastic analysis using the effectiveness factors
466 suggested by this study.

467 **ACKNOWLEDGEMENTS**

468 The authors wish to gratefully acknowledge the financial support of the UK Engineering and Physical
469 Sciences Research Council (EPSRC) through grant EP/I018972/1. The authors also wish to extend
470 their sincere thanks to the staff of the University of Cambridge Structures Research Lab for their
471 invaluable assistance in carrying out the experimental work reported above. Additional data related to
472 this publication is available at the University of Cambridge institutional data repository:
473 [<https://doi.org/10.17863/CAM.8477>]

474 **REFERENCES**

475 AASHTO (American Association of State Highway Transportation Officials) (2008). 'Bridging the
476 Gap: Restoring and Rebuilding the Nation's Bridges', Washington D.C.

477 ACI (American Concrete Institute) (2014). "Building Code Requirements for Structural Concrete and
478 Commentary", *ACI 318-14*, Farmington Hills, USA

479 Birkeland, P. W. and Birkeland, H. W. (1966) 'Connections in Precast Concrete Construction' *J. Am.*
480 *Concrete I., Proc.*, 63(3), pp. 345-368.

481 BSI (2004), EN 1992-1-1:2004 'Design of Concrete Structures. General Rules and Rules for
482 Buildings', BSI, London, UK

- 483 Chen, G. (1988) 'Plastic Analysis of Beams, Deep Beams and Corbels', *Structural Research Lab*
484 *Report No. R-237*, Technical University of Denmark, Copenhagen
- 485 Foster, R.M., Morley, C.T. and Lees, J. M. (2016) 'Modified Push-Off Testing of an Inclined Shear
486 Plane in Reinforced Concrete Strengthened with CFRP Fabric.' *J. Compos. Constr.*, 20(3),
487 04015061, 10.1061/(ASCE)CC.1943-5614.0000623
- 488 Gouvernement du Québec (2007), *Commission of Inquiry into the Collapse of a Portion of the de la*
489 *Concorde Overpass October 3, 2006 – October 15, 2007: Report*, Gouvernement du Québec
- 490 Hanson, N.W. (1960) 'Precast Prestressed Concrete Bridges 2: Horizontal Shear Connections',
491 *Journal of the PCA Research and Development Laboratories*, Vol. 2, No. 2, pp. 38-58
- 492 Highways Agency (2003) *Technical Audit of the Application of BA79: A Review Of Bridge*
493 *Assessment Failures on the Motorway and Trunk Road Network* [prepared by Shave, J., Denton,
494 S.R. and Charlton, M.], Highways Agency: Dorking
- 495 Hofbeck, J.A, Ibrahim, I.O. & Mattock, A.H. (1969) 'Shear Transfer in Reinforced Concrete', *Journal*
496 *of the American Concrete Institute: Proceedings*, Vol. 66, No. 2, pp. 119-128
- 497 Ibell, T.J., Morley, C.T. and Middleton, C.R. (1997) 'A Plasticity Approach to the Assessment of
498 Shear in Concrete Beam and Slab Bridges', *The Structural Engineer*, Vol. 75, No. 19, pp. 331-
499 338
- 500 Ibell, T. & Burgoyne, C. (1999) 'Use of Fiber-Reinforced Plastics Versus Steel for Shear
501 Reinforcement of Concrete', *ACI Structural Journal*, Vol. 96, No. 6, pp. 997-1002
- 502 Jensen, B.C. (1977) 'Some Applications of Plastic Analysis to Plain and Reinforced Concrete',
503 *Institute of Building Design Report No. 123*, Technical University of Denmark, Copenhagen
- 504 Mattock, A. H. and Hawkins, N. M. (1972). 'Shear Transfer In Reinforced Concrete – Recent
505 Research' *J. PCI*, Vol. 17, No. 2, pp. 55-75.

- 506 Mattock, A.H., Johal, L. and Chow, H.C. (1975) "Shear Transfer in Reinforced Concrete with
507 Moment or Tension Acting Across the Shear Plane" *J. PCI*, Vol. 20, No. 4, pp. 76-93.
- 508 Middleton, C.R. (2004) 'Bridge Management and Assessment in the UK' *Proceedings of Austroads*
509 *5th Bridge Conference*, Austroads, Australia, 16.
- 510 Neville, A.M. (2011) *Properties of Concrete* (5th Ed.), Harlow: Pearson Education Limited
- 511 Nielsen, M.P. and Hoang, L.C. (2011) *Limit Analysis and Concrete Plasticity* (3rd Ed.), CRC Press:
512 London
- 513 Santos, P.M.D. & Julio, E.N.B.S. (2012) 'A State-of-the-art Review on Shear-friction', *Engineering*
514 *Structures*, Vol. 45, pp. 435-448, <http://doi.org/10.1016/j.engstruct.2012.06.036>
- 515 Shave, J.D., Ibell, T.J. and Denton, S.R. (2007) 'Shear Assessment of Reinforced Concrete Bridges
516 with Short Anchorage Lengths', *The Structural Engineer*, Vol. 85, No. 5, pp. 30-37
- 517 Walraven, J.C. and Reinhardt, H.W. (1981) 'Theory and Experiments on the Mechanical Behaviour of
518 Cracks in Plain and Reinforced Concrete Subject to Shear Loading' *Heron*, No. 26, Vol. 1, pp.
519 1-68.
- 520 Zhang, J-P. (1997) 'Strength of Cracked Concrete, Part 2 –Micromechanical Modelling of Shear
521 Failure in Cement paste and in Concrete', *Structural Research Lab Report No. R-17*, Technical
522 University of Denmark, Copenhagen
- 523

524

525

526